Disentangling the roles of neocortical alpha/beta and hippocampal theta/gamma oscillations in human episodic memory formation

Benjamin J. Griffiths[1,2,3], María Carmen Martín-Buro[4,5], Bernhard P. Staresina[1,2], & Simon Hanslmayr[1,2,6]

1) School of Psychology, University of Birmingham, UK
2) Centre for Human Brain Health, University of Birmingham, UK
3) Department of Psychology, Ludwig-Maximilians-University Munich, Munich, Germany
4) Laboratory of Cognitive and Computational Neuroscience (UCM-UPM), Center for Biomedical Technology, 28223 Pozuelo de Alarcón, Madrid, Spain
5) Faculty of Health Sciences, King Juan Carlos University, 28922 Alcorcón, Madrid, Spain
6) Institute for Neuroscience and Psychology, University of Glasgow, UK

Contact Information / Corresponding Author

Simon Hanslmayr

simon.hanslmayr@glasgow.ac.uk

Abstract: 221 words

Main text: 1,801 words

Methods: 2,723 words

Number of figures: 3

Abstract

Episodic memory formation relies on at least two distinct capabilities: 1) our ability to process a vast amount of sensory information, and 2) our ability to bind these sensory representations together to form a coherent memory. The first process is thought to rely on a reduction in neocortical alpha/beta power, while the second is thought to be supported by hippocampal theta-gamma phase-amplitude coupling. However, most studies investigating human episodic memory use paradigms where the two cognitive capabilities overlap. As such, empirical support for the distinction of the two associated neural phenomena is lacking. Here, we addressed this by asking seventeen human participants (11 female, 6 male) to complete a sequence-learning paradigm that temporally separated information representation from mnemonic binding, while MEG recordings were acquired. We found that a decrease in neocortical alpha/beta power during the perception of the sequence correlated with enhanced memory performance. Similar power decreases during mnemonic binding, however, had no bearing on memory formation. In contrast, an increase in hippocampal theta/gamma phase-amplitude coupling during mnemonic binding correlated with enhanced memory performance, but similar coupling during sequence perception bared no relation to later memory performance. These results demonstrate that alpha/beta power decreases and hippocampal theta/gamma phase-amplitude coupling represent two temporally dissociable processes in episodic memory, with the former relating to information representation while the latter relates to mnemonic binding.

Introduction

An episodic memory is a personal detail-rich, long-term memory that is anchored to a unique point in time and space (Tulving, 2002). The formation and retrieval of these memories are thought to rely on neocortical alpha/beta desynchronisation and hippocampal theta/gamma synchronisation (Hanslmayr, Staresina, & Bowman, 2016), both of which are prevalent in a wide range of human episodic memory tasks (for reviews, see Hanslmayr & Staudigl, 2014; Nyhus & Curran, 2010).

Neocortical alpha/beta desynchrony is thought to be beneficial for information representation (Hanslmayr, Staudigl, & Fellner, 2012). This idea is derived from the tenets of information theory, which propose that unpredictable states (e.g. a desynchronised network, where the firing of one neuron cannot predict the firing of another) convey substantially more information than predictable states. In direct support of this idea, neocortical alpha/beta (8-20Hz) power decreases have been shown to correlate with the enhanced fidelity of neural representations present in BOLD signal (Griffiths, Mayhew, et al., 2019). Moreover, interfering with these power decreases via transcranial magnetic brain stimulation impairs both episodic memory formation and retrieval (Hanslmayr, Matuschek, & Fellner, 2014; Waldhauser, Braun, & Hanslmayr, 2016). Together, these findings (see also Fellner, Bäuml, & Hanslmayr, 2013; Long & Kahana, 2015; Martín-Buro, Wimber, Henson, & Staresina, 2020; Sederberg et al., 2007) suggest that alpha/beta power decreases are intimately related to the successful representation of information pertaining to episodic memories.

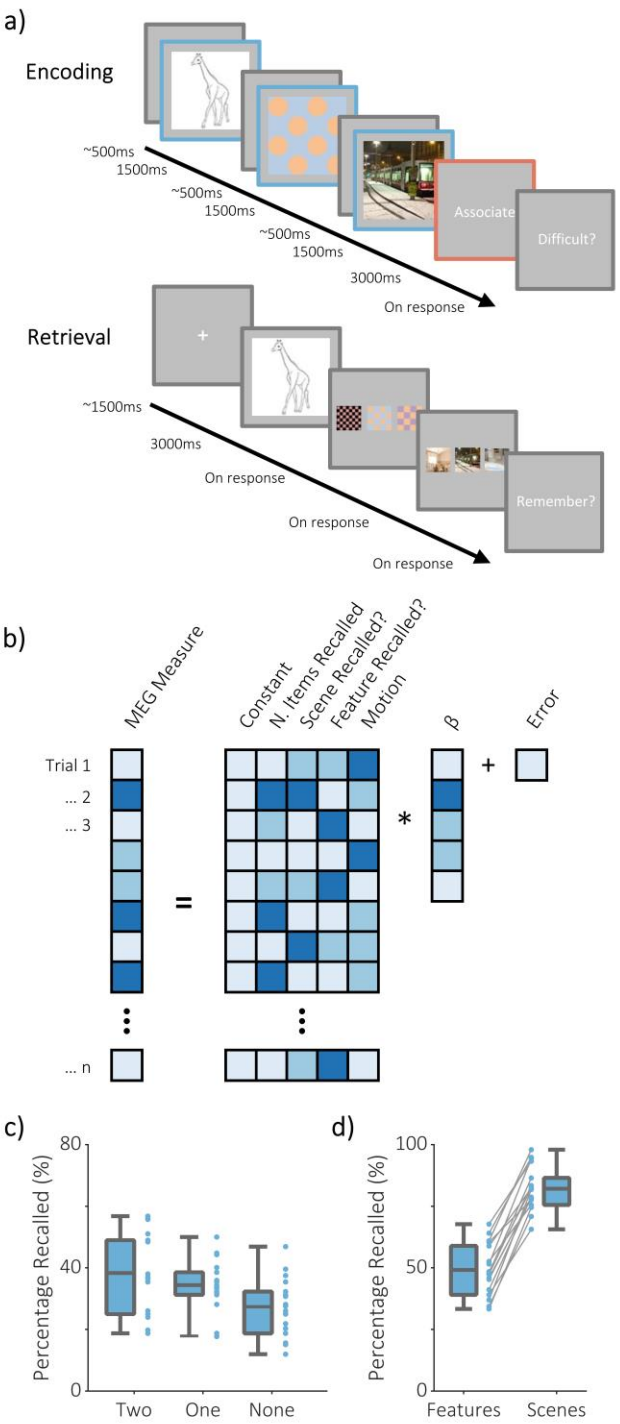

Figure 1. Overview of task, analytical approach and behavioural outcomes. (a) Paradigm schematic. Participants were presented with a sequence of three visual stimuli. The sequence always began with a line drawing of an object, and was then followed by a pattern and a scene (each with a brief fixation cross shown between). Participants were then given a short interval to create a mental image incorporating the three stimuli, before being asked to rate how difficult it was to create the association. After a distractor task, participants were presented with the object as a cue and asked to recall both the pattern and the scene, each from a choice of three stimuli. After selection, participants had to rate how confident they felt about their response. The epochs representing "sequence perception" are outlined in blue, and the epoch representing "mnemonic binding" is outlined in red. **(b)** Analysis schematic. Spectral power and theta-gamma phase-amplitude coupling were modelled using a general linear model including predictors for the number of items recalled, scene and feature memory recall, and head motion. The resulting standardised beta coefficient for the central predictor (i.e. number of items recalled) was extracted, pooled across participants, and subjected to a one sample t-test to determine whether the number of items recalled predicted changes in spectral power and/or theta-gamma coupling. **(c)** Boxplot depicting the number of items recalled for each participant. Participants, on average, correctly recalled both the associated pattern and associated scene on 38.3% of trials, recalled only one associated stimulus on 34.4% of trials, and failed to recall either associate on 27.3% of trials. **(d)** Boxplot depicting memory performance for each stimulus type. Participants correctly recalled the associated pattern on 49.2% of trials, and correctly recalled the associated scene on 82.1% of trials (both of which are well above chance performance [33.3%]). A paired-samples t-test revealed that memory for scenes was substantially greater than memory for patterns ($p < 0.001$, Cohen's $d_z = 4.31$).

Hippocampal theta and gamma oscillations also play a pivotal role in episodic memory formation (e.g. Bahramisharif, Jensen, Jacobs, & Lisman, 2018; Heusser, Poeppel, Ezzyat, & Davachi, 2016; Staudigl & Hanslmayr, 2013; Tort, Komorowski, Manns, Kopell, & Eichenbaum, 2009). The phase of theta is thought to determine whether long-term potentiation (LTP) or long-term depression (LTD) occurs (Hasselmo, Bodelón, & Wyble, 2002), and gamma synchronisation compliments this process by driving neurons to fire at the frequency optimal for spike-timing dependent plasticity (STDP; Bi & Poo, 1998; Jutras, Fries, & Buffalo, 2009; Nyhus & Curran, 2010). In combining these two phenomena, hippocampal theta-gamma phase-amplitude

coupling is well-positioned to facilitate the binding of information into a coherent memory trace (Hanslmayr et al., 2016; Lisman & Jensen, 2013).

On a cognitive level however, many paradigms probing human episodic memory formation involve substantial overlap in information representation and mnemonic binding, making it difficult to conclude that their associated neural phenomena are truly dissociable. Here, we addressed this problem by using a paradigm that temporally separates these cognitive processes. Seventeen participants were briefly presented with a sequence of three stimuli (always consisting of an object, a feature and a scene), and then given a small window to intentionally bind these stimuli together for a later associative memory test. We hypothesised that (1) neocortical alpha/beta power decreases are most prevalent during the perception of the sequence (from here on termed "sequence perception"), as this requires extensive processing of the details of each item prior to binding, and (2) hippocampal theta-gamma phase-amplitude coupling is most prevalent when participants intentionally associate the stimuli together (from here on termed "mnemonic binding), given that theta-gamma coupling is a proxy for forms of long-term potentiation. Indeed, the results reported below support these hypotheses, suggesting that neocortical alpha/beta desynchrony and hippocampal theta/gamma synchrony relate to dissociable processes in episodic memory formation.

Results

Neocortical alpha/beta power decreases during sequence perception predict enhanced memory performance

We first investigated the extent to which spectral power fluctuates as a function of memory performance during sequence perception. We hypothesised that, as information relating to the three stimuli needs to be processed to form a complete memory, alpha/beta power should decrease with enhanced memory performance. To test this, the time-series of sensor-level MEG gradiometer data was decomposed into spectral power using 6-cycle Morlet wavelets (for low frequencies; 2-40Hz) and Slepian multitapers (for high frequencies; 40-100Hz), with the 1/f component subtracted by means of linear modelling (Manning, Jacobs, Fried, & Kahana, 2009; Zhang & Jacobs, 2015). Spectral power was then entered as an outcome variable into a multiple regression with four predictor variables: the number of items recalled, whether the scene was recalled, whether the pattern was recalled, and head motion. The first regressor was of primary interest, while the latter three were used to attenuate potentially confounding variables. The resulting beta coefficients for the regressor of interest were pooled across participants and entered into a group-level, cluster-based one-sample t-test which compared observed values against the null hypothesis (t=0; Maris & Oostenveld, 2007).

Cluster-based analysis revealed a significant effect where power decreases correlated with an increase in memory performance (p_{corr} = 0.035, Cohen's d_z = 0.60, cluster size = 1013, summed cluster t-statistic = -2499.07; see figure 2a-c). This cluster extended over the posterior sensors, bilaterally, between 8 and 15Hz (see figure 2a-b). No similar decrease was observed during mnemonic binding (p_{corr} = 0.124).

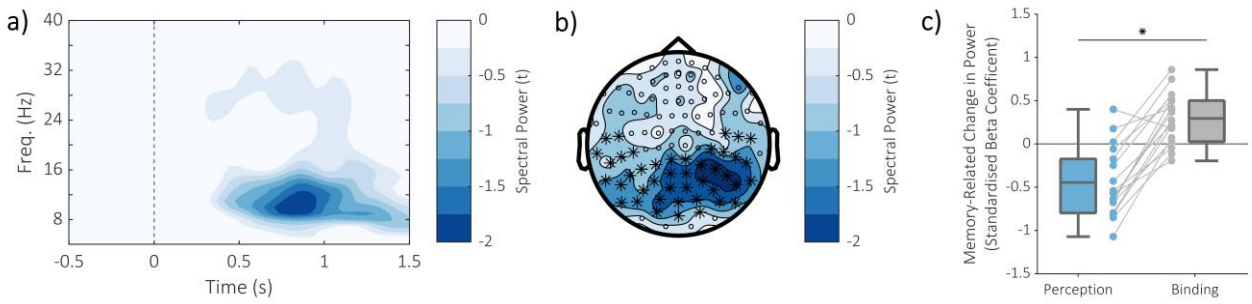

Figure 2. Alpha/beta power decreases during sequence perception correlate with increased memory performance. (a) Time-frequency representation depicting fluctuation in power as a function of number of items recalled, averaged across all sensors within the significant cluster. During perception, a significant alpha/beta power decrease accompanies enhanced performance during the memory test. **(b)** Topographic plot of post-stimulus alpha/beta power (0.5-1.5s; 8-15Hz) as a function of number of items recalled during test. Black crosses indicate sensors that were part of the significant cluster. **(c)** Boxplots depicting alpha/beta power during perception and mnemonic binding, as a function of items recalled. Alpha/beta power decreases during sequence perception correlated with memory performance to a significantly greater degree than alpha/beta power decreases during mnemonic binding.

A direct contrast of spectral power between sequence perception and mnemonic binding demonstrated that the inverse relationship between alpha power and memory performance was significantly more pronounced during perception, relative to mnemonic binding (p_{corr} = 0.021, Cohen's d_z = 0.62, cluster size = 1098, cluster t-statistic = -2799.90). Together, these findings suggest that memory-related decreases in alpha/beta power correlate with ongoing visual perception, and not mnemonic binding.

Hippocampal theta/gamma phase-amplitude coupling during mnemonic binding, but not information representation, predicts successful episodic memory formation

We then probed how hippocampal theta/gamma phase-amplitude coupling relates to episodic memory formation. Using source-reconstructed data, we first extracted the theta and gamma peaks in the hippocampal power spectrum for each participant individually. Across participants, the peak in hippocampal theta arose at 5.0Hz (standard deviation: 0.9Hz; range: 3.7-6.6Hz; when searching between 2 and 7Hz), while the peak hippocampal gamma frequency arose at 67.0Hz (standard deviation: 8.8Hz; range: 55.9-85.0Hz; when searching between 40 and 100Hz). By taking the peak frequencies for each participant (theta filtered ±0.5Hz around peak; gamma filtered ±10Hz around peak), we ensured that analysis focused on the coupling between two oscillatory signals (Aru et al., 2014). The modulation index (Tort, Komorowski, Eichenbaum, & Kopell, 2010) was computed to provide a measure of phase-amplitude coupling. These resulting modulation index values underwent the statistical analysis as was conducted for alpha/beta power in the previous section.

During mnemonic binding, increases in theta/gamma phase-amplitude coupling correlated with enhanced subsequent memory performance (t(16) = 2.53, p = 0.011, Cohen's d_z = 0.61; see figure 3). No significant coupling was observed during perception (p > 0.5). A direct contrast in PAC between these two epochs suggests that memory-related increases in PAC are more pronounced during mnemonic binding

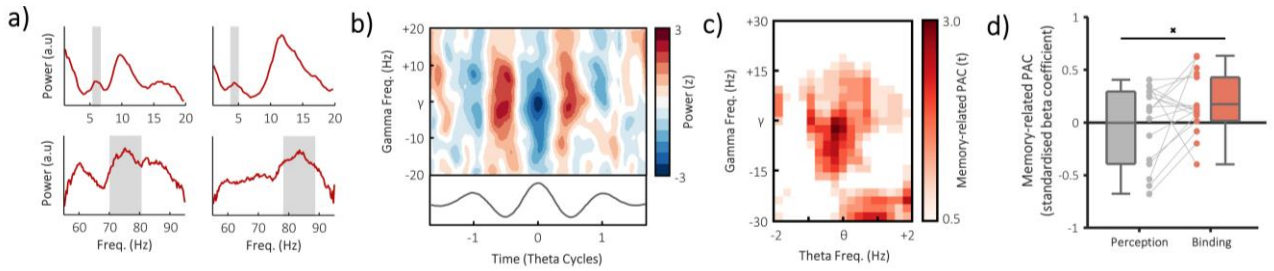

Figure 3. Increases in hippocampal theta/gamma coupling during mnemonic binding correlate with increased memory performance. **(a)** two exemplars of participant-specific hippocampal theta peaks (top) and gamma peaks (bottom) identified in 1/f-corrected power spectra. The shaded area depicts the identified peak ± 0.5Hz for theta and ± 5Hz for gamma. **(b)** the modulation of peak gamma power (γ) as a function of peak theta phase across all trials. Peak gamma appears to decrease during the peaks of the theta phase and increase during troughs of the theta phase. **(c)** the specificity of memory-related hippocampal theta-gamma phase-amplitude coupling. The plot is centred on participant-specific peak theta (θ) and peak gamma (γ) frequencies and extends from γ-30 to γ+30 on the γ-axis, and θ-2 to θ+2 on the x-axis. **(d)** boxplot depicting the fit between memory performance and hippocampal theta-gamma coupling during perception and binding. Hippocampal theta-gamma coupling during binding correlates with memory performance to a significantly greater degree than expected by chance, and to a greater degree than during sequence perception.

relative to sequence perception (t(16) = 1.72, p = 0.053, Cohen's d_z = 0.42). These results suggest that memory-related theta/gamma phase-amplitude coupling is most prominent during periods of mnemonic binding.

To confirm the spatial specificity of the effect observed during mnemonic binding, we re-ran this analysis using four additional regions of interest: the frontal lobe, parietal lobe, temporal lobe (excluding the hippocampus), and the occipital lobe. None of these regions exhibited significant theta-gamma phase-amplitude coupling during mnemonic binding (frontal: p = 0.308, parietal: p = 0.250, temporal: p = 0.078, occipital: p = 0.169). These results suggest the memory-related enhancement in theta/gamma phase-amplitude coupling predominately arises in the hippocampus.

Disentangling the roles of neocortical alpha/beta and hippocampal theta/gamma activity in human episodic memory

Lastly, we formalised the distinction between memory-related neocortical alpha/beta power decreases and hippocampal theta-gamma phase-amplitude coupling. To this end, we conducted a 2x2 repeated measures ANOVA with cogntive task (perception vs. binding) and metric (alpha/beta power decreases vs. theta-gamma coupling) as factors. This revealed a significant interaction where memory-related alpha/beta power decreases and memory-related theta-gamma coupling increases are dependent on the nature of the ongoing cognitive task [F(1,16) = 10.79, p = 0.005, partial eta squared = 0.40]. There was no main effect of cognitive task [F(1,16) = 0.80, p = 0.39, partial eta squared = 0.05], nor metric [F(1,16) = 0.14, p > 0.5, partial eta squared < 0.01]. These results suggest that a double dissociation exists between neocortical alpha/beta power decreases and hippocampal theta-gamma phase-amplitude coupling, with the former being most pronounced during periods of information processing and the latter being most pronounced during periods of mnemonic binding.

Discussion

Reductions in neocortical alpha/beta power and enhancements in hippocampal theta-gamma phase-amplitude coupling are thought to play dissociable roles in the formation of episodic memories (Hanslmayr et al., 2016). However, most studies investigating human episodic memory use paradigms in which these two phenomena co-occur, meaning empirical support for the dissociation of these processes is lacking. Here, we addressed this by using a paradigm that temporally separated information representation (thought to be supported by alpha/beta power decreases) and mnemonic binding (thought to be supported by hippocampal theta-gamma coupling). In line with our hypotheses, we found that memory-related decreases in neocortical alpha/beta power uniquely arose during sequence perception, while memory-related increases in hippocampal theta/gamma phase-amplitude coupling uniquely arose during the mnemonic binding. Together, these results suggest that alpha/beta power decreases and hippocampal theta/gamma synchronisation reflect two distinct cognitive processes in episodic memory formation.

The representation of information relating to a to-be-encoded memory is thought to be supported by neocortical alpha/beta power decreases (Hanslmayr et al., 2012). Information theory proposes that unpredictable states, such as desynchronised neural networks, carry more information than predictable states (Shannon & Weaver, 1949). In line with this hypothesis, we found that memory-related reductions in alpha/beta power (an index for neural desynchrony) only arose when participants were required to process information about a sequence, and not when the sequence was being bound together (i.e. when no further information was presented for processing). The restriction of alpha/beta power decreases to time points where information can be processed adds further support to the idea that alpha/beta power decreases correlate with the representation of information relevant to episodic memories (Griffiths, Mayhew, et al., 2019; Hanslmayr et al., 2012).

During mnemonic binding, hippocampal theta-gamma phase-amplitude coupling scaled with memory performance. Mechanistically speaking, these increases may reflect a heightened degree of long-term potentiation (LTP) within the hippocampus. By coupling gamma oscillations resonating at a frequency optimal for spike-timing dependent plasticity (STDP; Bi & Poo, 1998; Nyhus & Curran, 2010) to the phase of theta optimal for LTP (Hasselmo et al., 2002), the potential for building synaptic connections between hippocampal neurons is increased greatly. Based on such ideas, one could speculate that the memory-related theta-gamma coupling observed during the binding window reflects the transformation of the three discrete sequence stimuli into a singular cohesive episodic memory. Similarly, the absence of memory-related theta-gamma coupling during sequence perception may be attributable to the fact that the sequence is still unfolding, and, as such, a cohesive representation of all three stimuli cannot yet be formed. Notably, this is not to say that no theta-gamma coupling unfolds during sequence perception (indeed, several frameworks and empirical studies propose the opposite; Bahramisharif, Jensen, Jacobs, & Lisman, 2018; Griffiths & Fuentemilla, 2019; Heusser, Poeppel, Ezzyat, & Davachi, 2016; Lisman & Jensen, 2013), but rather, any theta-gamma coupling that does

190 arise during that window is not predictive of later memory performance in this particular task. Perhaps instead,
191 such coupling is predictive of item-context binding (e.g. Howard & Kahana, 2002), a measure not assessable
192 here.

193 If these two phenomena are dissociable, does this mean that they act in complete independence of one
194 another during encoding? Here, we would argue "no". Mnemonic binding cannot occur if the relevant
195 information has not been perceived, as there is no information to bind. Therefore, one could expect that the
196 underlying neural correlates of mnemonic binding are also contingent on the prior neural processing of
197 relevant information. In line with such ideas, prior work has shown that the magnitude of hippocampal gamma
198 synchronisation can be predicted by preceding neocortical alpha/beta power decreases (Griffiths, Parish, et
199 al., 2019). Integrating this finding with the current results, one could speculate that neocortical desynchrony
200 and hippocampal synchrony are correlated with distinct cognitive processes (as evidenced above), but both
201 neural phenomena (and the associated cognitive processes) must arise and interact to create and episodic
202 memory.

203 In sum, these results demonstrate that decreases in neocortical alpha/beta power and increases in
204 hippocampal theta/gamma phase-amplitude coupling are functionally dissociable in episodic memory
205 formation (Hanslmayr et al., 2016).

206 Materials and Methods

207 *Participants*

208 Twenty-eight participants were recruited (mean age = 25.4; age range = 20-33; 68% female; 82% right-handed).
209 These participants received course credit or financial reimbursement in return for their participation. One participant was
210 excluded for excessive head movement (greater than 2 standard deviations above group mean). Four participants were
211 excluded for poor data quality (more than 50% of trials rejected for artifacts). Six participants were excluded for extreme
212 memory performance (fewer than 15 trials in one of the three memory conditions). This left seventeen participants for
213 further analysis (mean age = 24.9; age range = 20-32; 65% female; 82% right-handed). Ethical approval was granted by
214 the Research Ethics Committee at the University of Birmingham (ERN_15-0335), complying with the Declaration of
215 Helsinki.

216 *Experimental design*

217 Each participant completed a visual associative memory task (see figure 1a). During encoding, participants were
218 presented with a line drawing of an object, a pattern, and a scene (each for 1500ms, with a jittered 600ms (±100ms)
219 fixation cross shown between each stimulus). Participants were then given a short interval to create a mental image
220 incorporating the three stimuli to help them recall the stimuli for a later memory test. Participants were then asked to
221 rate how difficult they found associating the triad. This question was used to keep participants attending to the task,
222 rather than provide a meaningful metric for analysis. The next trial began after the participant had responded to the
223 difficulty question. After associating 48 triads, participants started the distractor task. In the distractor task, participants
224 attended to a fixation cross in the centre of a black screen. The fixation cross would flash momentarily (~100ms) from
225 light grey to either white or dark grey approximately every 20 seconds. The participants were instructed to count the

number of times the fixation cross changed to white (ignoring the times it turned dark grey) and report this value at the end of the task (approximately 2.5mins later). The retrieval task followed the distractor. Here, participants were presented with the line drawing (for 3000ms) and asked to recall the mental image they made during the encoding phase. Then, participants were presented with three patterns (one correct and two lures) and asked to identify the pattern associated with the line drawing. After responding, participants were presented with three scenes (one correct and two lures) and again asked to identify the pattern associated with the line drawing. After responding, participants were then asked to indicate how confident they were about their choices. They could select 'guess' (i.e. they guessed their choice), 'unsure' (i.e. they could not remember the item, but had a feeling it was the correct choice), or 'certain' (i.e. they could vividly remember the item). Participants were asked to recall all 48 triads learnt in the earlier encoding phase.

Participants completed four blocks of this task (192 trials in total). The order in which the pattern and scene were presented during perception was swapped between each block (where a "block" is defined as a complete cycle of encoding, distractor and retrieval tasks). On blocks where scenes preceded patterns during perception, the presentation order at retrieval was also reversed.

For all responses, participants used two non-magnetic, single-finger optical response pads. The left pad allowed participants to cycle through the possible responses, and the right pad allowed participants to confirm their selection.

Behavioural analysis

For each trial, memory performance was coded as either 'complete' (i.e. they remembered both the scene and the pattern), 'partial' (i.e. they remembered only one of the associates), or 'forgotten' (i.e. they remembered neither the scene nor the pattern). Any selection where the participant indicated that they guessed was marked as a 'miss'.

MEG acquisition

MEG data was recorded using a 306-channel (204 gradiometers, 102 magnetometers) whole brain Elekta Neuromag TRIUX system (Elekta, Stockholm, Sweden) in a magnetically shielded room. Participants were placed in the supine position for the duration of the experiment. Data was continuously recorded at a sampling rate of 1000Hz. The head shape of each participant (including nasion and left/right ear canal) was digitised prior to commencing the experiment. Continuous head position indicators (cHPI) were recorded throughout. The frequencies emitted by the cHPI coils were 293Hz, 307Hz, 314Hz and 321Hz. Magnetometer data was excluded from the main analysis as they contained substantial noise that could not be effectively removed or attenuated.

MEG preprocessing

All data analysis was conducted in Matlab using Fieldtrip (Oostenveld, Fries, Maris, & Schoffelen, 2011) in conjunction with custom scripts. First, the data was lowpass filtered at 165Hz to remove the signal generated by the HPI coils. Second, the data was epoched around each event of interest. At encoding, the epochs reflected the time windows where each stimulus was presented (from here on termed 'sequence perception') and when the 'associate' prompt was presented (termed 'mnemonic binding'). Sequence perception epochs began 2000ms before stimulus onset and ended 3500ms after onset (that is, 2000ms after stimulus offset). Mnemonic binding epochs began 2000ms before stimulus onset and ended 4500ms after onset (that is, 2000ms after stimulus offset). Third, independent components analysis was conducted, and any identifiable eye-blink or cardiac components were removed. Fourth, the data was visually inspected, and any artefactual epochs or sensors were removed from the dataset (mean percentage of trials removed: 18.0%; range: 5.7-32.2%).

Movement correction

To identify participants with extreme head motion during MEG recordings, the recorded data was first highpass filtered to 250Hz to isolate the cHPI signal. Second, the variance of the signal for each sensor was computed across every time point of the continuous recording. Third, the variance was mean averaged across sensors to provide a singular estimate of change in cHPI signal across the duration of the experiment. Fourth, the mean variance and its standard deviation was calculated across participants. Lastly, participants with extreme head motion were identified as those with variance greater than two standard deviations above the group mean. These participants were excluded from further analysis.

To help attenuate motion-related confounds in the spectral power and phase-amplitude coupling analyses, a trial-by-trial estimate of motion was calculated. First, the data was highpass filtered at 250Hz. Second, the data was epoched into trials matching those outlined in the section above. Third, the envelope of the signal in each epoch was calculated (to avoid issues of mean phase angle difference in cHPI signal across trials). Fourth, the envelope was averaged over time to provide a single value for each epoch and channel. Fifth, the dot product was computed across sensors between the first epoch and every other epoch (algebraically: $\sum_{i=1}^{n} a_i\, b_i$, where *n* is the number of channels, a_i is the power at sensor i during the first trial, and b_i is the power at sensor i during the trial of interest). This provided a single value (between zero and infinity) for each trial that described how similar the topography of that trial was to the first trial – the higher the value, the more similar the topographies are between the two trials (with the assumption that the more dissimilar a cHPI topography is to the starting topography, the more the head has deviated from its starting position). These values were entered as a regressor of no interest in the central multiple regression analyses.

Time-frequency decomposition and statistical analysis

Sensor-level time-frequency decomposition was conducted on the sequence perception and mnemonic binding epochs. For low frequencies, the preprocessed data was first convolved with a 6-cycle wavelet (-0.5 to 3 seconds [to 2 seconds for perceptual epochs to avoid the subsequent stimulus], in steps of 50ms; 2 to 40Hz; in steps of 1Hz). For high frequencies, Slepian multitapers were first used to estimate power (-0.5 to 3 seconds [to 2 seconds for perceptual epochs], in steps of 50ms; 40 to 100Hz, in steps of 4Hz). For this latter analysis, frequency smoothing was set to one quarter of the frequency of interest and temporal smoothing was set to 200ms. Second, planar gradiometers were combined by summing the power of the vertical and horizontal components. Third, for perceptual trials only, power was then averaged over the three stimulus presentation windows of each triad to provide mean power during perception of the triad. Any triads where one or more epochs had been rejected during preprocessing were excluded at this stage. We averaged spectral power across the three windows as we reasoned that this approach would be most sensitive to changes in spectral power that predicted the number of items later recalled. To successfully recall a stimulus, an alpha/beta power decrease must arise in two of the windows – the initial line drawing (i.e. the retrieval cue) and the to-be-recalled stimulus. As such, focusing analyses on a single stimulus is less sensitive to later memory performance than an aggregate measure created by averaging across the epochs. Fourth, the background 1/f characteristic was subtracted using an iterative linear fitting procedure.

To isolate oscillatory contributions, 1/f activity was attenuated in the time-frequency data by subtracting the linear fit of the 1/f characteristic (Griffiths, Parish, et al., 2019; Manning et al., 2009; Zhang & Jacobs, 2015). To this end, a vector containing values of each derived frequency (*A*) and another vector containing the power spectrum, averaged over all time-points and trials of the relevant memory condition (*B*) were log-transformed to approximate a linear function. The

linear equation $Ax = B$ was solved using least-squares regression, where x is an unknown constant describing the 1/f characteristic. The 1/f fit (Ax) was then subtracted from the log-transformed power spectrum (B). As this fit can be biased by outlying peaks (Haller et al., 2018), an iterative algorithm was used that removed probable peaks and then refitted the 1/f. Outlying peaks in this 1/f-subtracted power spectrum were identified using a threshold determined by the mean value of all frequencies that sat below the linear fit. The MEG power spectrum is the summation of the 1/f characteristic and oscillatory activity (i.e. at no point does oscillatory activity subtract from the 1/f), therefore all values that sit below the linear fit can be seen an estimate error of the fit. Any peaks that exceed the threshold were removed from the general linear model, and the fitting was repeated. Notably, as power for the low frequencies (2-40Hz) and high frequencies (40-100Hz) was calculated using different methods (wavelets and Slepian multitapers, respectively), the two bands have disparate levels of temporal and spectral smoothing. To avoid a spurious fitting due of the 1/f because of these differences, the 1/f correction was conducted separately for these two bands.

For statistical analysis, a trial-based multiple regression was run for each participant. Four regressors were used to predict observed power for every channel x frequency x time point independently. These four regressors were (1) number of items recalled, (2) whether the scene was recalled, (3) whether the pattern was recalled, (4) the change in head position [based on the motion calculation outlined above]. The first regressor was of primary interest, the second and third regressors isolated spectral power changes that can be uniquely described by whether the scene/pattern was recalled (respectively), and the fourth regressor accounted for changes in spectral power driven by head movement (see the next paragraph for notes on multicollinearity). The beta weight of the first regressor, obtained for a given channel x frequency x time point, was then standardised by dividing the standard error of the fit (providing a t-value) to attenuate the impact of poor model fits on the final analysis. Here, a positive standardised beta coefficient would indicate that spectral power increases with more items recalled, and a negative beta coefficient would indicate that spectral power decreases with more items recalled. The beta coefficients for each participant were pooled across the sample and entered into a one-tailed cluster-based permutation test (2000 permutations, alpha threshold = 0.05, cluster alpha threshold = 0.05, minimum neighbourhood size = 3; Maris & Oostenveld, 2007) to examine whether the observed fits consistently deviated from the null hypothesis (t=0) across participants. Clusters that produced a p-value less than 0.05 were considered significant. Cohen's d_z was used as the measure of effect size for these clusters (Lakens, 2013), where $d_z = \frac{\bar{t}}{\sqrt{n}}$, $\bar{t}$ = mean t-statistic within the cluster, n = number of participants.

Notably, it is plausible to suggest that the three memory regressors are, to some extent, correlated and that this would introduce multicollinearity into the regression models. To test this, we calculated the Variance Inflation Factor (VIF) – a measure of the magnitude of multicollinearity. Rule of thumb suggests that a VIF greater than 10 is considered high and could compromise the model (Kutner, Nachtsheim, & Neter, 2004). The VIF between number of items recalled and scene recall success was, on average, 2.615 (s.d. 2.621), and the VIF between number of items recalled and pattern recall success was, on average, 1.027 (s.d. 0.033). As these values fall below the threshold of 10, multicollinearity is not an apparent concern.

Source analysis

The preprocessed data was reconstructed in source space using individual head models and structural (T1-weighted) MRI scans for all but two individuals who did not wish to return for an MRI scan. For these two individuals, a standard head model and MRI scan was used (taken from the Fieldtrip toolbox; for details, see http://www.fieldtriptoolbox.org/template/headmodel). The head shape (together with the HPI coil positions) of each

participant was digitised using a Polhemus Fasttrack system. The timelocked MEG data was reconstructed using a single-shell forward model and a Linearly Constrained Minimum Variance beamformer (LCMV; van Veen, van Drongelen, Yuchtman, & Suzuki, 1997). The lambda regularisation parameter was set to 1%.

MEG phase-amplitude coupling computation and statistical analysis

To calculate the extent to which hippocampal gamma activity coupled to hippocampal theta phase, the modulation index (MI) was calculated (Tort et al., 2010). First, the peak theta and gamma frequencies were calculated by estimating power across all hippocampal virtual sensors (bilaterally, as defined by the automated anatomical labelling [AAL] atlas) using the same time-frequency decomposition method reported above. The Matlab function *findpeaks()* was then used to extract the most prominent peak within the theta (2-7Hz) and gamma (40-100Hz) bands for each participant. Across participants, the mean theta peak was at 5.0Hz (standard deviation: 0.9Hz; range: 3.7-6.6Hz), and the mean gamma peak was at 67.0Hz (standard deviation: 8.8Hz; range: 55.9-85.0Hz). Second, the time-series of the hippocampal virtual sensors were duplicated, with the first being filtered around the theta peak (±0.5Hz) and the second being filtered around the gamma peak (±5Hz). Third, the Hilbert transform was applied to the theta- and gamma-filtered time-series, with the phase of the former and power of the latter being extracted. Fourth, the time-series data was re-epoched, beginning 500ms after the onset of the stimulus/fixation cross and ending 500ms before the onset of the next screen. This attenuated the possibility that an event-related potential and/or edge artifacts from the filtering/Hilbert transform could influence the phase-amplitude coupling measure (Aru et al., 2014). Fifth, gamma power was binned into 12 equidistant bins of 30°, according to the concurrent theta phase. This binning was conducted for each trial and sensor separately. Sixth, the MI was computed by comparing the observed distribution to a uniform distribution. Seventh, the resulting MI values were subjected to a trial-based multiple regression conducted in the same manner as for the spectral power analyses. However, two additional regressors were added to this model: (1) hippocampal peak theta power [per trial, averaged across 500ms to 2500ms], (2) hippocampal peak gamma power [per trial, averaged across 500ms to 2500ms]. These regressors addressed the potential confound of concurrent power influence phase estimates (Aru et al., 2014). Eighth, these results were averaged over hippocampal virtual sensors and these per-participant standardised beta coefficients were subjected to a permutation-based one-sample t-test contrasting memory-related changes in phase-amplitude coupling to the null hypothesis (t=0). Notably, as we had focused our analyses on the peak theta and gamma frequencies, and used the average PAC values across virtual sensors, only a single statistical comparison was made. Therefore, no cluster-based multiple comparison correction was required. Note that the p-values reported here are estimated by permutation rather than from the parametric test, therefore, the t-values and degrees of freedom we report should only be used for reference.

To test the spatial specificity of this effect, the same pipeline was used to assess theta-gamma phase-amplitude coupling in the frontal, occipital, parietal and temporal lobes (individually; defined in by in *wfupickatlas* toolbox for SPM).

References

Aru, J., Priesemann, V., Wibral, M., Lana, L., Pipa, G., Singer, W., & Vicente, R. (2014). Untangling cross-frequency coupling in neuroscience. *Current Opinion in Neurobiology*, *31*(September 2014), 51–61. https://doi.org/10.1101/005926

Bahramisharif, A., Jensen, O., Jacobs, J., & Lisman, J. (2018). Serial representation of items during working memory maintenance at letter-selective cortical sites. *PLoS Biology*, 171660. https://doi.org/10.1101/171660

Bi, G., & Poo, M. (1998). Synaptic modifications in cultured hippocampal neurons: Dependence on spike timing, synaptic strength, and postsynaptic cell type. *Journal of Neuroscience*, *18*(24), 1–9. https://doi.org/10.1038/25665

Fellner, M.-C., Bäuml, K.-H. T., & Hanslmayr, S. (2013). Brain oscillatory subsequent memory effects differ in power and long-range synchronization between semantic and survival processing. *NeuroImage*, *79*, 361–370. https://doi.org/10.1016/j.neuroimage.2013.04.121

Griffiths, B. J., & Fuentemilla, L. (2019). Event conjunction: How the hippocampus integrates episodic memories across event boundaries. *Hippocampus*, 1–15. https://doi.org/10.1002/hipo.23161

Griffiths, B. J., Mayhew, S. D., Mullinger, K. J., Jorge, J., Charest, I., Wimber, M., & Hanslmayr, S. (2019). Alpha/beta power decreases track the fidelity of stimulus-specific information. *ELife*, *8*(e49562), 1–22. https://doi.org/10.32470/ccn.2019.1199-0

Griffiths, B. J., Parish, G., Roux, F., Michelmann, S., Plas, M. Van Der, Kolibius, D., … Hanslmayr, S. (2019). Directional coupling of slow and fast hippocampal gamma with neocortical alpha/beta oscillations in human episodic memory. *Proceedings of the National Academy of Sciences*, 1–9. https://doi.org/10.1073/pnas.1914180116

Haller, M., Donoghue, T., Peterson, E., Varma, P., Sebastian, P., Gao, R., … Voytek, B. (2018). Parameterizing neural power spectra. *BioRxiv*, 299859. https://doi.org/10.1101/299859

Hanslmayr, S., Matuschek, J., & Fellner, M.-C. (2014). Entrainment of prefrontal beta oscillations induces an endogenous echo and impairs memory formation. *Current Biology*, *24*(8), 904–909. https://doi.org/10.1016/j.cub.2014.03.007

Hanslmayr, S., Staresina, B. P., & Bowman, H. (2016). Oscillations and episodic memory – Addressing the synchronization/desynchronization conundrum. *Trends in Neurosciences*, *39*(1), 16–25. https://doi.org/10.1016/j.tins.2015.11.004

Hanslmayr, S., & Staudigl, T. (2014). How brain oscillations form memories--a processing based perspective on oscillatory subsequent memory effects. *NeuroImage*, *85 Pt 2*, 648–655. https://doi.org/10.1016/j.neuroimage.2013.05.121

Hanslmayr, S., Staudigl, T., & Fellner, M.-C. (2012). Oscillatory power decreases and long-term memory: the

information via desynchronization hypothesis. *Frontiers in Human Neuroscience*, *6*(74), 1–12. https://doi.org/10.3389/fnhum.2012.00074

Hasselmo, M. E., Bodelón, C., & Wyble, B. P. (2002). A proposed function for hippocampal theta rhythm: Separate phases of encoding and retrieval enhance reversal of prior learning. *Neural Computation*, *14*(4), 793–817. https://doi.org/10.1162/089976602317318965

Heusser, A. C., Poeppel, D., Ezzyat, Y., & Davachi, L. (2016). Episodic sequence memory is supported by a theta-gamma phase code. *Nature Neuroscience*, *19*(August). https://doi.org/10.1038/nn.4374

Howard, M. W., & Kahana, M. J. (2002). A distributed representation of temporal context. *Journal of Mathematical Psychology*, *46*(3), 269–299. https://doi.org/10.1006/jmps.2001.1388

Jutras, M. J., Fries, P., & Buffalo, E. A. (2009). Gamma-Band Synchronization in the Macaque Hippocampus and Memory Formation. *Journal of Neuroscience*, *29*(40), 12521–12531. https://doi.org/10.1523/JNEUROSCI.0640-09.2009

Kutner, M. H., Nachtsheim, C. J., & Neter, J. (2004). *Applied Linear Regression Models* (4th ed.). McGraw-Hill Irwin.

Lakens, D. (2013). Calculating and reporting effect sizes to facilitate cumulative science: A practical primer for t-tests and ANOVAs. *Frontiers in Psychology*, *4*(NOV). https://doi.org/10.3389/fpsyg.2013.00863

Lisman, J. E., & Jensen, O. (2013). The theta-gamma neural code. *Neuron*, *77*(6), 1002–1016. https://doi.org/10.1016/j.neuron.2013.03.007

Long, N. M., & Kahana, M. J. (2015). Successful memory formation is driven by contextual encoding in the core memory network. *NeuroImage*, *119*, 332–337. https://doi.org/10.1016/j.neuroimage.2015.06.073

Manning, J. R., Jacobs, J., Fried, I., & Kahana, M. J. (2009). Broadband shifts in local field potential power spectra are correlated with single-neuron spiking in humans. *Journal of Neuroscience*, *29*(43), 13613–13620. https://doi.org/10.1523/JNEUROSCI.2041-09.2009

Maris, E., & Oostenveld, R. (2007). Nonparametric statistical testing of EEG- and MEG-data. *Journal of Neuroscience Methods*, *164*(1), 177–190. https://doi.org/10.1016/j.jneumeth.2007.03.024

Martín-Buro, M. C., Wimber, M., Henson, R. N., & Staresina, B. P. (2020). Alpha rhythms reveal when and where item and associative memories are retrieved. *Journal of Neuroscience*, *40*(12), 2510–2518. https://doi.org/10.1523/JNEUROSCI.1982-19.2020

Nyhus, E., & Curran, T. (2010). Functional role of gamma and theta oscillations in episodic memory.

Neuroscience and Biobehavioral Reviews, *34*(7), 1023–1035. https://doi.org/10.1016/j.neubiorev.2009.12.014

Oostenveld, R., Fries, P., Maris, E., & Schoffelen, J.-M. (2011). FieldTrip: Open source software for advanced analysis of MEG, EEG, and invasive electrophysiological data. *Computational Intelligence and Neuroscience*, *2011*, 1–9. https://doi.org/10.1155/2011/156869

Sederberg, P. B., Schulze-Bonhage, A., Madsen, J. R., Bromfield, E. B., McCarthy, D. C., Brandt, A., … Kahana, M. J. (2007). Hippocampal and neocortical gamma oscillations predict memory formation in humans. *Cerebral Cortex*, *17*(5), 1190–1196. https://doi.org/10.1093/cercor/bhl030

Shannon, C. E., & Weaver, W. (1949). *A mathematical theory of communication*. Urbana, IL: University of Illinois Press.

Staudigl, T., & Hanslmayr, S. (2013). Theta oscillations at encoding mediate the context-dependent nature of human episodic memory. *Current Biology*, *23*(12), 1101–1106.

Tort, A. B. L., Komorowski, R., Eichenbaum, H., & Kopell, N. (2010). Measuring phase-amplitude coupling between neuronal oscillations of different frequencies. *Journal of Neurophysiology*, *104*(2), 1195–1210. https://doi.org/10.1152/jn.00106.2010

Tort, A. B. L., Komorowski, R. W., Manns, J. R., Kopell, N. J., & Eichenbaum, H. (2009). Theta-gamma coupling increases during the learning of item-context associations. *Proceedings of the National Academy of Sciences*, *106*(49), 20942–20947. https://doi.org/10.1073/pnas.0911331106

Tulving, E. (2002). Episodic memory: from mind to brain. *Annual Review of Psychology*, *53*, 1–25. https://doi.org/10.1146/annurev.psych.53.100901.135114

van Veen, B., van Drongelen, W., Yuchtman, M., & Suzuki, A. (1997). Localization of brain electrical activity via linearly constrained minimum variance spatial filtering. *IEEE Transactions on Biomedical Engineering*, *44*(9), 867–880. https://doi.org/10.1109/10.623056

Waldhauser, G. T., Braun, V., & Hanslmayr, S. (2016). Episodic memory retrieval functionally relies on very rapid reactivation of sensory information. *Journal of Neuroscience*, *36*(1), 251–260. https://doi.org/10.1523/JNEUROSCI.2101-15.2016

Zhang, H., & Jacobs, J. (2015). Traveling theta waves in the human hippocampus. *Journal of Neuroscience*, *35*(36), 12477–12487. https://doi.org/10.1523/JNEUROSCI.5102-14.2015